



**HAL**  
open science

## Mutation of the Arabidopsis NRT1.5 nitrate transporter causes defective root-to-shoot nitrate transport.

Shan-Hua Lin, Hui-Fen Kuo, Geneviève Canivenc, Choun-Sea Lin, Marc Lepetit, Po-Kai Hsu, Pascal Tillard, Huey-Ling Lin, Ya-Yun Wang, Chyn-Bey Tsai, et al.

### ► To cite this version:

Shan-Hua Lin, Hui-Fen Kuo, Geneviève Canivenc, Choun-Sea Lin, Marc Lepetit, et al.. Mutation of the Arabidopsis NRT1.5 nitrate transporter causes defective root-to-shoot nitrate transport.. The Plant cell, 2008, 20 (9), pp.2514-28. 10.1105/tpc.108.060244 . hal-00356462

**HAL Id: hal-00356462**

**<https://hal.science/hal-00356462>**

Submitted on 31 May 2020

**HAL** is a multi-disciplinary open access archive for the deposit and dissemination of scientific research documents, whether they are published or not. The documents may come from teaching and research institutions in France or abroad, or from public or private research centers.

L'archive ouverte pluridisciplinaire **HAL**, est destinée au dépôt et à la diffusion de documents scientifiques de niveau recherche, publiés ou non, émanant des établissements d'enseignement et de recherche français ou étrangers, des laboratoires publics ou privés.

# Mutation of the *Arabidopsis* *NRT1.5* Nitrate Transporter Causes Defective Root-to-Shoot Nitrate Transport

Shan-Hua Lin,<sup>a</sup> Hui-Fen Kuo,<sup>a</sup> Geneviève Canivenc,<sup>b</sup> Choun-Sea Lin,<sup>a,1</sup> Marc Lepetit,<sup>b</sup> Po-Kai Hsu,<sup>a</sup> Pascal Tillard,<sup>b</sup> Huey-Ling Lin,<sup>c</sup> Ya-Yun Wang,<sup>a</sup> Chyn-Bey Tsai,<sup>a</sup> Alain Gojon,<sup>b</sup> and Yi-Fang Tsay<sup>a,2</sup>

<sup>a</sup> Institute of Molecular Biology, Academia Sinica, Taipei 11529, Taiwan

<sup>b</sup> Biochimie et Physiologie Moléculaire des Plantes, Unité Mixte de Recherche 5004, Agro-M/Centre National de la Recherche Scientifique/L'Institut National de la Recherche Agronomique/Université Montpellier 2, 34060 Montpellier, Cedex 1, France

<sup>c</sup> Department of Horticulture, National Chung Hsing University, Taichung 40227, Taiwan

Little is known about the molecular and regulatory mechanisms of long-distance nitrate transport in higher plants. *NRT1.5* is one of the 53 *Arabidopsis thaliana* nitrate transporter *NRT1* (Peptide Transporter *PTR*) genes, of which two members, *NRT1.1* (*CHL1* for Chlorate resistant 1) and *NRT1.2*, have been shown to be involved in nitrate uptake. Functional analysis of cRNA-injected *Xenopus laevis* oocytes showed that *NRT1.5* is a low-affinity, pH-dependent bidirectional nitrate transporter. Subcellular localization in plant protoplasts and in planta promoter- $\beta$ -glucuronidase analysis, as well as in situ hybridization, showed that *NRT1.5* is located in the plasma membrane and is expressed in root pericycle cells close to the xylem. Knockdown or knockout mutations of *NRT1.5* reduced the amount of nitrate transported from the root to the shoot, suggesting that *NRT1.5* participates in root xylem loading of nitrate. However, root-to-shoot nitrate transport was not completely eliminated in the *NRT1.5* knockout mutant, and reduction of *NRT1.5* in the *nrt1.1* background did not affect root-to-shoot nitrate transport. These data suggest that, in addition to that involving *NRT1.5*, another mechanism is responsible for xylem loading of nitrate. Further analyses of the *nrt1.5* mutants revealed a regulatory loop between nitrate and potassium at the xylem transport step.

## INTRODUCTION

Nitrate and ammonium ions are the two major nitrogen sources for higher plants. Due to its toxicity, ammonium is preferentially assimilated in the root and then transported in an organic form to the aerial parts. By contrast, nitrate can be assimilated into ammonium and then amino acids in the root or shoot. Partitioning of nitrate assimilation between the root and shoot depends on the plant species, external nitrate concentration, temperature, and light intensity (reviewed in Smirnov and Stewart, 1985). If there is sufficient light, nitrate assimilation in the leaf has a lower energy cost than in the root. However, some disadvantages of leaf nitrate assimilation include (1) if light is limited, nitrate assimilation and carbon dioxide fixation will compete directly for the reductants and ATP generated by photosynthetic electron transport (Canvin and Atkins, 1974), and (2) hydroxyl ions generated in the leaf need to be neutralized by the synthesis of organic acids (in the root, the pH balance may possibly be

maintained by reducing proton excretion or increasing bicarbonate excretion). Due to these factors, the partition of nitrate assimilation between the root and shoot shows both seasonal and diurnal fluctuations, allowing the plant to sustain maximal growth. In turn, the partition of nitrate assimilation depends on the partition of nitrate between the root and shoot.

To transport nitrate to the aerial parts of the plant, nitrate has to be loaded into the xylem vessels of the root vascular stele. In *Arabidopsis thaliana* roots, four layers of cells are found surrounding the xylem, these being the epidermis, cortex, endodermis, and pericycle (in the order external to internal). In the endodermis, a band of the radial cell wall, called the Casparian strip, is impregnated with the wax-like hydrophobic substance, suberin, which restricts water and ion diffusion in the apoplast. The presence of the Casparian strip means that ions have to cross the membrane and the plant can use two regulated processes to control what ions, and how much of each, can be loaded into the xylem. First, to be loaded into the xylem, ions in the soil solution need to enter the symplast (cytoplasmic) stream for radial transport through the outer cell layers of the root before they encounter the Casparian band. This entry into the symplast stream occurs via channels and transporters in the plasma membrane of the epidermis, cortex, and outer half of the endodermis. Transport through the cytoplasm allows the ions to pass through the endodermal cells that are surrounded by the Casparian strip, thus allowing transport into the xylem. Second, ions moving in the symplast stream and reaching the parenchyma around the xylem vessels need to move across the plasma

<sup>1</sup> Current address: Agriculture Biotechnology Research Center, Academia Sinica, Taipei 11529, Taiwan.

<sup>2</sup> Address correspondence to yftsay@gate.sinica.edu.tw.

The author responsible for distribution of materials integral to the findings presented in this article in accordance with the policy described in the Instructions for Authors (www.plantcell.org) is: Yi-Fang Tsay (yftsay@gate.sinica.edu.tw).

 Online version contains Web-only data.

 Open Access articles can be viewed online without a subscription. www.plantcell.org/cgi/doi/10.1105/tpc.108.060244



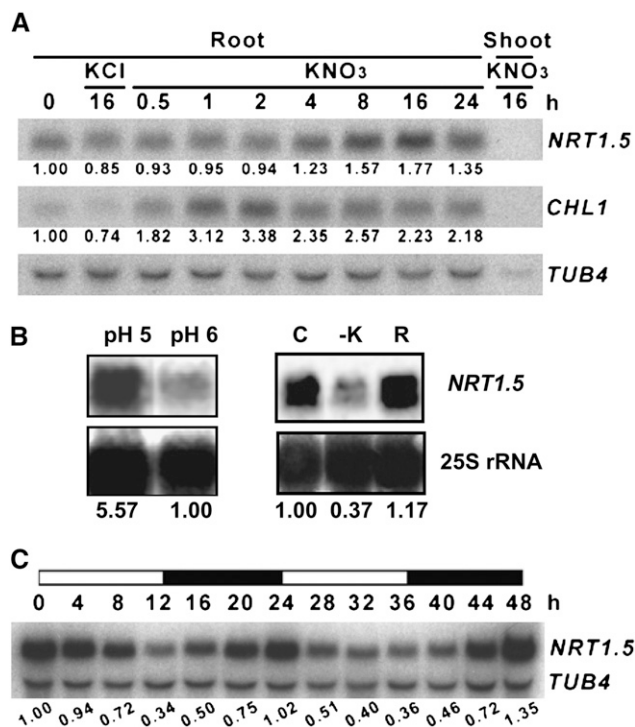


**Figure 2.** Expression of *NRT1.5* Is Regulated by Nitrate, pH, Potassium, and Diurnally.

**(A)** Time-course analysis of *NRT1.5* expression following nitrate induction. Plants were grown on agarose plates with 2.5 mM  $(\text{NH}_4)_2$  succinate for 10 d and then shifted to plates with 5 mM  $\text{KNO}_3$  or KCl for the indicated time, and then total RNA (10  $\mu\text{g}$ ) was isolated from leaf or root tissues. After electrophoresis, the RNA was transferred to a Hybond N membrane (Amersham) and hybridized with  $^{32}\text{P}$ -radiolabeled DNA probes for *NRT1.5*, *NRT1.1* (*CHL1*), or the tubulin (*TUB4*) gene. The values for *NRT1.5* and *NRT1.1* mRNA levels normalized to *TUB4* mRNA levels, with the 0 h levels set at 1.0, are indicated below the blots.

**(B)** Effect of external pH and potassium limitation on *NRT1.5* transcript accumulation in the roots. For the pH experiment, 1 week before harvest, 7-week-old hydroponically grown plants were transferred to the nutrient solution B buffered with 4.4 mM MES (pH 5 or 6, with Tris added to the buffer for pH 6). For the potassium limitation experiment, 8-week-old plants grown hydroponically in the complete nutrient solution B were used directly (lane C) or, after washing the roots in 0.1 mM  $\text{CaSO}_4$ , were transferred for 48 h to a potassium-free nutrient solution (potassium substituted by sodium) and either tested directly (lane -K) or resupplied for a further 48 h with complete nutrient solution B (lane R). The plants were grown under an 8/16-h light/dark cycle and harvested at the same time in the middle of the light period. Total RNA was analyzed by RNA gel blotting using  $^{32}\text{P}$ -radiolabeled DNA probes for *NRT1.5* mRNA or 25S rRNA as described previously (Loque et al., 2003). *NRT1.5* mRNA levels normalized to 25S rRNA levels, with the levels at pH 6.0 or in complete nutrient (lane C) set at 1.0, are indicated below the blots.

**(C)** Diurnal regulation of *NRT1.5* expression. Total RNA (10  $\mu\text{g}$ ) was isolated from root tissues of plants grown under a 12/12-h light/dark cycle on agarose plates with 5 mM  $\text{NH}_4\text{NO}_3$  at pH 5.5 for 10 d. After electrophoresis, the RNA was transferred to a Hybond N membrane and hybridized with  $^{32}\text{P}$ -radiolabeled DNA probes for *NRT1.5* and the tubulin (*TUB4*) gene. *NRT1.5* mRNA levels normalized to *TUB4* mRNA levels, with the 0 h levels set as 1.0, are indicated below the blots.

nitrate uptake (Huang et al., 1999), while *NRT2.1* and *NRT2.2* are only involved in high-affinity nitrate uptake (Filleur et al., 2001). The identification of the genes responsible for different components of nitrate uptake has facilitated the study of the complicated regulatory network involved and its role in plant development (Guo et al., 2001; Munos et al., 2004; Little et al., 2005; Remans et al., 2006).

To date, knowledge of nitrate xylem loading has mainly been obtained from electrophysiological studies. Based on the negative membrane potentials of plant cells ( $-50$  to  $-200$  mV) and the nitrate concentration observed in xylem exudates (1 to 50 mM), it is believed that nitrate entry into the xylem is probably passive (Glass and Siddiqi, 1995). Electrophysiological studies have identified several types of anion conductance in protoplasts prepared from the xylem parenchyma of barley (*Hordeum vulgare*) and maize (*Zea mays*; Köhler and Raschke, 2000; Gilliam and Tester, 2005). Two of these, an inwardly rectifying anion channel (X-IRAC) and a quickly activating anion conductance (X-QUAC), are nitrate permeable and may be involved in the xylem loading of nitrate. Further studies have shown that X-IRAC and X-QUAC are differentially regulated by water stress (Gilliam and Tester, 2005) and that the voltage dependence of X-QUAC is regulated by apoplastic nitrate, suggesting that xylem loading of nitrate is subject to delicate regulation (Köhler et al., 2002).

Little is known about the molecular identity of carriers involved in the long-distance root-to-shoot transport of nitrate. In this study, we show that one of the *Arabidopsis* NRT1 genes, *NRT1.5*, is involved in this process.

## RESULTS

### Cloning and Sequence Analysis of *NRT1.5*

*NRT1.5* (At1g32450) was identified by a homology search comparing the amino acid sequence of *NRT1.1* (*CHL1*) with the EST database for *Arabidopsis*. Using the EST clone identified (clone ID 36F6T7) as a probe, a full-length clone (*pAtNRT1.5*) was isolated from an *Arabidopsis* cDNA library (Elledge et al., 1991) constructed in the  $\lambda$ YES vector. The deduced protein sequence of *NRT1.5* showed 36% identity with *CHL1* and 31% identity with *NRT1.2* (Figure 1). Like all members of the NRT1 family, *NRT1.5* was found to contain 12 putative transmembrane domains and a long hydrophilic loop between transmembrane domains 6 and 7.

### Pattern of Expression of *NRT1.5* in Response to Nitrate Induction, pH Change, Potassium Limitation, and Diurnal Regulation

As shown in Figure 2, *NRT1.5*, like *CHL1* (*NRT1.1*) and *NRT1.2*, was found to be preferentially expressed in the root and, like *CHL1*, was also nitrate-inducible. However, the response to nitrate was much slower for *NRT1.5* than for *CHL1*. As shown in

For **(A)** to **(C)**, similar results were obtained in at least two other experiments. Different exposures were taken to ensure that the quantification was in the linear range.

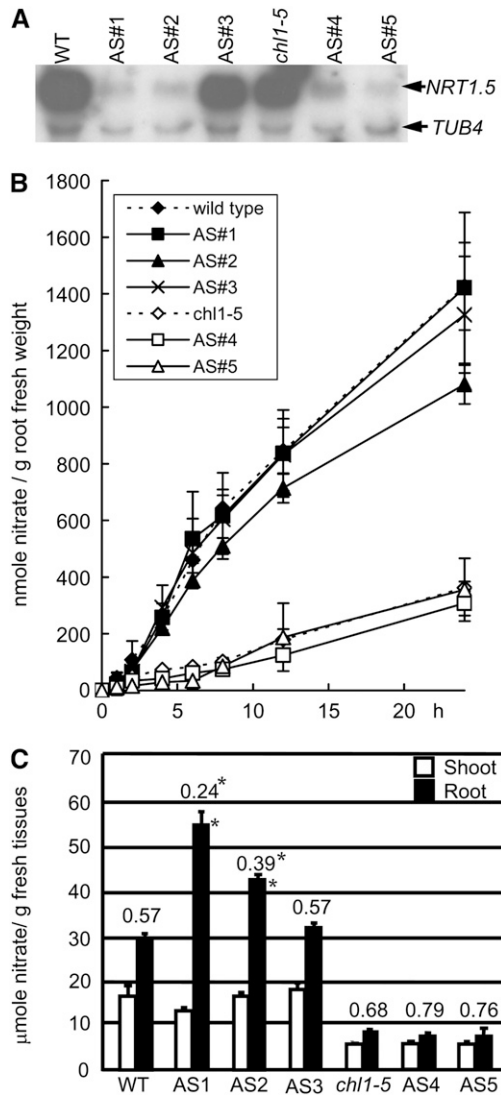


**Figure 3.** Antisense *NRT1.5* Plants Show Decreased Nitrate Translocation to the Shoot.

**(A)** *NRT1.5* mRNA levels in transgenic plants containing antisense *NRT1.5*. Total RNA (10  $\mu$ g) was isolated from root tissues of plants grown on agarose plates with 12.5 mM  $(\text{NH}_4)_2$  succinate for 2 weeks and then shifted to medium with 25 mM  $\text{KNO}_3$  for 16 h. After electrophoresis and transfer to a Hybond N membrane, the RNA was hybridized with a  $^{32}\text{P}$ -radiolabeled antisense *NRT1.5* riboprobe at 75°C and then with an  $^{32}\text{P}$ -radiolabeled DNA probe for the tubulin (*TUB4*) gene at 65°C. Anti-*NRT1.5* #1, #2, and #3 (AS#1, #2, and #3) are three independent transgenic plants containing antisense *NRT1.5* on the wild-type background, while anti-*NRT1.5* #4 and #5 (AS#4 and #5) are two independent plants containing antisense *NRT1.5* on the *chl1-5* mutant background.

**(B)** Nitrate uptake activities of antisense *NRT1.5* plants. Seedlings were grown in the nutrient solution A containing 12.5 mM  $\text{NH}_4\text{NO}_3$  for 2 weeks and then the plants were washed and transferred to medium containing 8 mM  $\text{KNO}_3$  for the uptake assay. The amount of nitrate depleted from the medium was measured at the time points indicated. The experiment shown was performed in triplicate, and the error bars represent the SD. The traces for the wild type and AS#1 overlap. Similar results were obtained in two other experiments.

Figure 2A and reported previously (Tsay et al., 1993; Huang et al., 1999), when plants are shifted from ammonium medium to nitrate medium, *CHL1* mRNA levels begin to increase within 30 min, reach a maximum 2 to 4 h after the shift, then begin to decline. By contrast, in this study, *NRT1.5* mRNA levels were unchanged 4 h after the shift and only began to increase at 8 h (Figure 2A).

In addition, as shown in Figure 2B, *NRT1.5* expression was downregulated by a pH increase. It was also downregulated by potassium limitation; when potassium was replaced by sodium, *NRT1.5* expression was  $\sim 37\%$  of control levels (Figure 2B), and when it was replaced by calcium, *NRT1.5* expression was  $\sim 60\%$  of control levels (see Supplemental Figure 1 online), showing that *NRT1.5* is downregulated by potassium limitation but that the presence of sodium may have an additional effect.

*NRT1.5* expression during the 12/12-h diurnal cycle was also examined. As shown in Figure 2C, *NRT1.5* mRNA levels gradually decreased and increased during the light and dark period, respectively, being maximal at the end of the dark period.

### Transgenic Plants Expressing Antisense-*NRT1.5* Are Defective in Transporting Nitrate from the Root to the Shoot

To investigate the *in vivo* function of *NRT1.5*, an antisense *NRT1.5* construct was introduced into both the wild-type Columbia (Col) ecotype and the nitrate uptake-defective mutant *chl1-5* (*nrt1.1-5*) (Tsay et al., 1993). Three homozygous transgenic plants (AS#1, #2, and #3) containing antisense *NRT1.5* in the wild-type background and two (AS#4 and #5) in the *chl1-5* background were isolated and confirmed by genomic DNA gel blot hybridization analysis and kanamycin segregation. RNA gel blot analysis using an *NRT1.5* antisense riboprobe showed that *NRT1.5* mRNA levels were significantly reduced in AS#1, AS#2, AS#4, and AS#5 but remained at wild-type levels in AS#3 (Figure 3A). To determine their nitrate net uptake activities, nitrate depletion of the medium by 2-week-old plants was monitored for 24 h. Compared with the parental lines, the low-affinity nitrate uptake activity of the antisense plants was either unaffected or only slightly reduced (Figure 3B). Thus, unlike *NRT1.1* (*CHL1*) (Huang et al., 1996; Touraine and Glass, 1997) and *NRT1.2* (Huang et al., 1999), *NRT1.5*, although also expressed in the root, is not involved in nitrate uptake.

**(C)** Root and shoot nitrate contents of antisense *NRT1.5* plants. Seedlings were grown on lifted mesh with only the roots submerged in the nutrient solution A containing 12.5 mM  $\text{NH}_4\text{NO}_3$  for 1 week and then were shifted to medium containing 12.5 mM  $(\text{NH}_4)_2$  succinate for another week to deplete internal nitrate. Nitrate concentrations at the end of ammonium incubation were  $<0.7$   $\mu\text{mole/g}$  tissue in the root and 1.3  $\mu\text{mole/g}$  in the shoot. To determine nitrate partitioning in the root and shoot, plants were transferred to medium containing 8 mM  $\text{KNO}_3$  for 16 h and then the amount of nitrate in the root and shoot was determined using HPLC. The white and black bars represent the nitrate concentration in the shoot and root, respectively. The number above the bar is the shoot/root nitrate concentration ratio. The experiment was performed in triplicate, and the error bars represent the SD. \*,  $P < 0.01$  compared with the wild-type values for AS#1-3 or the *chl1-5* values for AS#4 and #5. Similar results were obtained in three other experiments.

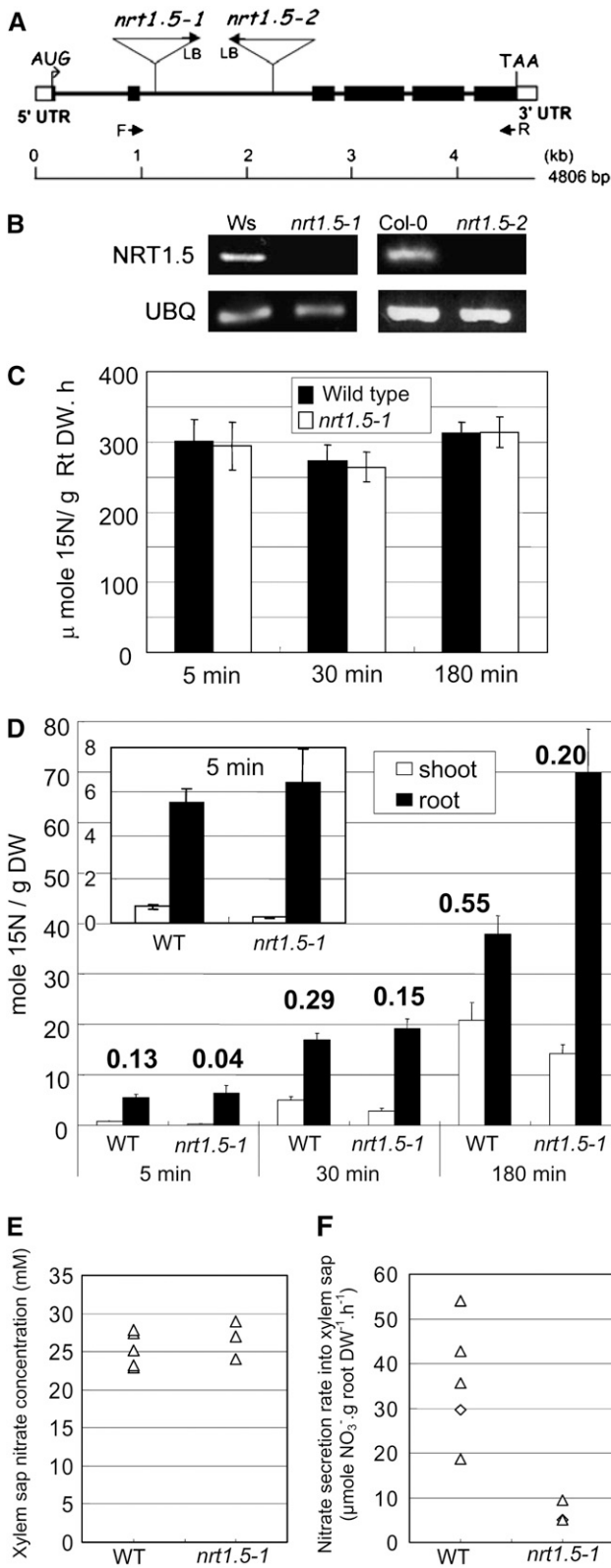


**Figure 4.** The T-DNA-Inserted Mutants *nrt1.5-1* and *nrt1.5-2* Also Show Decreased Nitrate Translocation to the Shoot.

The role of *NRT1.5* was then addressed by measuring the root and shoot nitrate contents of plants grown on lifted mesh. To deplete internal nitrate, 1-week-old  $\text{NH}_4\text{NO}_3$ -grown plants were shifted to  $(\text{NH}_4)_2$  succinate medium for another week, then root and shoot nitrate contents were determined after exposing the 2-week-old plants to 8 mM  $\text{KNO}_3$  for 16 h. As shown in Figure 3C, correlating well with the *NRT1.5* mRNA levels, the shoot/root nitrate concentration ratio was 0.57 in the wild type and AS#3 but was reduced to 0.24 and 0.39, respectively, in AS#1 and AS#2. This indicates that in AS#1 and AS#2, but not AS#3, more nitrate was retained in root tissue and less nitrate was found in the shoot. In AS#1 and AS#2, the nitrate increase in the root was more obvious than the decrease in the shoot. This might be explained by some of the nitrate transported to the shoot already being assimilated. On the other hand, as a consequence of the nitrate uptake defect in *chl1-5*, the nitrate content in plants on the *chl1-5* background (*chl1-5* itself and AS#4 and #5) was much lower than in plants with a wild-type background (wild type,

**(A)** Schematic map of the *nrt1.5* and *nrt1.5-2* mutants carrying a single copy of the T-DNA insert in the second intron of the *NRT1.5* gene. The black and white boxes represent the coding and untranslated regions (UTR), respectively. The arrows indicate the annealing positions of the primers used for genomic PCR or RT-PCR. F, *NRT1.5* forward primer; R, *NRT1.5* reverse primer; LB, T-DNA left border primer.

**(B)** RT-PCR analysis of *NRT1.5* mRNA levels in the wild-type and the homozygous *nrt1.5* mutants. Total RNA isolated from root tissue was analyzed by 25 cycles of RT-PCR using primers F and R. The presence of equal amount of cDNA in each reaction was verified by amplification with *UBQ* primers (bottom image, 23 cycles).

**(C)** Nitrate uptake activity of the *nrt1.5-1* mutant. Seedlings were grown on lifted mesh in the nutrient solution A containing 5 mM  $\text{NH}_4\text{NO}_3$  for 10 d and then were transferred to a nutrient solution with 4 mM  $\text{NH}_4^{15}\text{NO}_3$  for the indicated time and the amount of  $^{15}\text{N}$  taken into the plants measured. The experiment shown was performed with eight replicates, and the error bars represent the SD. No difference between the wild type and mutant was detected ( $P > 0.05$ ). Similar results were obtained in two other experiments. DW, dry weight.

**(D)** Root and shoot  $^{15}\text{N}$  contents of homozygous *nrt1.5-1* mutant. Seedlings were grown hydroponically in the nutrient solution B containing 5 mM  $\text{NH}_4\text{NO}_3$  for 8 weeks and then were transferred to complete nutrient solution with 4 mM  $\text{NH}_4^{15}\text{NO}_3$  for the indicated time. At the end of labeling, shoot and root tissues were collected separately and their  $^{15}\text{N}$  content analyzed using an isotope ratio mass spectrometer coupled with a carbon nitrogen elemental analyzer. Experiments were performed with 8 to 12 replicates. The white and black bars represent the  $^{15}\text{N}$  concentration in the shoot and root, respectively. The number above the bar is the shoot/root nitrate concentration ratio. Compared with the wild type, the shoot/root nitrate concentration ratios for all the time points tested were lower in the *nrt1.5-1* mutant ( $P < 0.01$  using Student's *t* test). The inset shows an enlarged figure for the 5 min experiment. The error bars represent the SD. Similar results for the *nrt1.5-2* mutant are shown in Supplemental Figure 2 online.

**(E)** and **(F)** Nitrate concentration in the xylem sap **(E)** and nitrate secretion rate into the xylem sap **(F)**. Seedlings were grown hydroponically for 8 weeks as described in **(D)** and then the shoots were excised under the rosette and the xylem exudate collected for 2.5 h as described previously (Gaynard et al., 1998; Takano et al., 2002). The volume and nitrate concentration of the xylem exudate were determined to calculate the nitrate secretion rate into xylem.

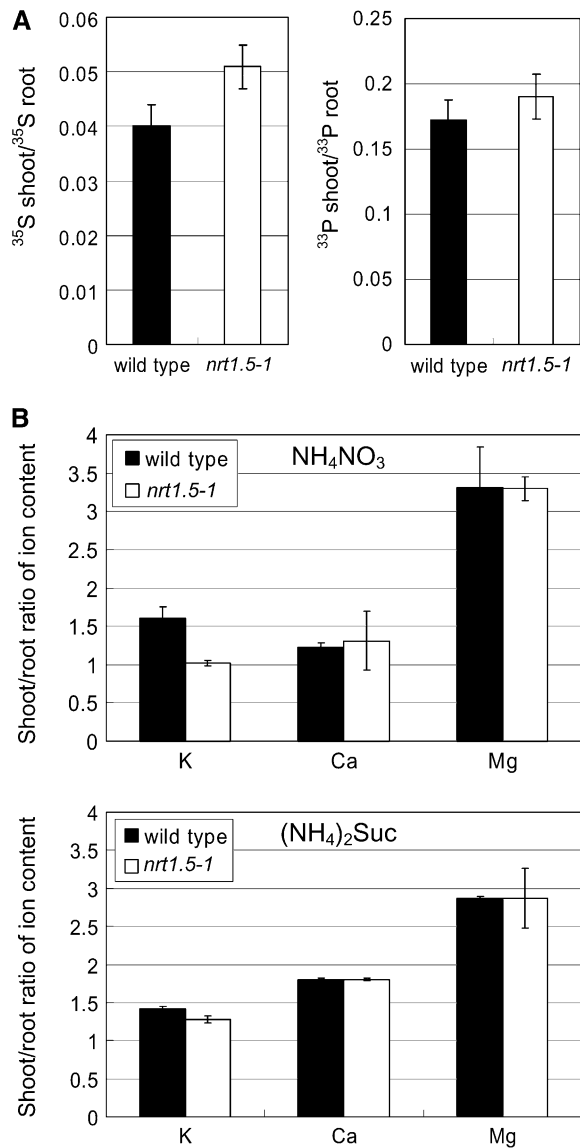


**Figure 5.** The Distribution of Potassium, Sulfate, Phosphate, Calcium, and Magnesium in *nrt1.5-1*.

**(A)** S translocation (left) and P translocation (right) of the *nrt1.5-1* mutant. Plants were grown hydroponically under the same conditions used for  $^{15}\text{N}$  translocation in Figure 4D and then were labeled for 30 min in nutrient solution containing either  $^{35}\text{SO}_4^{2-}$  or  $^{33}\text{PO}_4^{3-}$  and the radioactivity in root and shoot extracts measured using a scintillation counter. The results presented are the shoot/root ratio for the S (or P) concentration ( $\mu\text{mole/g}$  dry weight). There was no significant difference between the wild type and the *nrt1.5* mutant ( $P > 0.05$ ).

**(B)**  $\text{K}^+$ ,  $\text{Ca}^{2+}$ , and  $\text{Mg}^{2+}$  translocation of the *nrt1.5-1* mutant grown on lifted mesh with only the roots submerged in the nutrient solution A with  $\text{NH}_4\text{NO}_3$  (top) or  $(\text{NH}_4)_2$  succinate (bottom) as the nitrogen source. The potassium, calcium, and magnesium contents of the root and shoot tissue of 2-week-old plants were analyzed by atomic absorption spectrophotometer. The results presented are the shoot/root ion concentration ratio ( $\mu\text{g/mg}$  dry weight). Compared with the wild type, the ratio for potassium is lower in *nrt1.5-1* when the plants were grown with  $\text{NH}_4\text{NO}_3$  ( $P < 0.05$  based on Student's *t* test).

AS#1, #2, and #3) (Figure 3C). Interestingly, when the tissue nitrate content was low, blocking *NRT1.5* expression did not affect the root and shoot nitrate distribution (i.e., the root and shoot nitrate concentrations in AS#4 and #5 were similar to those in their parental line, *chl1-5*). Taken together, the results for these antisense plants show that *NRT1.5* is important for transporting nitrate from the root to shoot but is not the sole mechanism responsible for long-distance nitrate transport.

### The T-DNA-Tagged Mutants *nrt1.5-1* and *nrt1.5-2* Are Defective in Long-Distance Transport of Nitrate but Not of Sulfate or Phosphate

To further confirm the role of *NRT1.5* in long-distance nitrate transport, a T-DNA-tagged mutant *nrt1.5-1* in the Wassilewskija (Ws) ecotype was isolated by PCR-based screening (Krysan et al., 1999) and a second T-DNA-tagged mutant *nrt1.5-2* in the Col ecotype was obtained from the European Arabidopsis Stock Center. In both mutants, a T-DNA was inserted in the second intron (Figure 4A). No expression of *NRT1.5* mRNA was detected by RT-PCR analysis (Figure 4B), showing that both mutants were null mutants. Short-term nitrate uptake and translocation were analyzed by exposing the plants to  $\text{NH}_4^{15}\text{NO}_3$  for 5, 30, or 180 min. Consistent with the phenotype of the antisense plants, the nitrate uptake activity of the *nrt1.5-1* mutant was comparable to, or only slightly lower than, that in the wild type (Figure 4C). However, the amount of  $^{15}\text{N}$  translocated to the shoot was reduced in the mutant (Figure 4D). Five minutes after labeling with  $^{15}\text{N}$ -labeled nitrate, the shoot/root  $^{15}\text{N}$  concentration ratio was  $\sim 0.13$  in the wild type but only  $\sim 0.04$  in the mutant. After longer exposure, more and more  $^{15}\text{N}$  was translocated to the shoot, but the shoot/root  $^{15}\text{N}$  concentration ratio of the *nrt1.5-1* mutant was consistently lower than that of the wild type (Figure 4D). Reduced root-to-shoot  $^{15}\text{N}$  translocation was also observed in the second T-DNA-tagged mutant *nrt1.5-2* (see Supplemental Figure 2 online).

To confirm that *nrt1.5* mutants are defective in xylem transport of nitrate, xylem exudates of plants grown under the same hydroponic conditions as in the  $^{15}\text{N}$  translocation assay were collected and analyzed. The nitrate concentration of the xylem sap in the *nrt1.5* mutant was similar to that in the wild type (Figure 4E). However, due to a reduction in the secretion rate of the xylem exudates, the rate of nitrate secretion into the xylem sap was much lower in the mutant (Figure 4F). Xylem exudates were also collected from plants grown in soil and irrigated with 10 mM  $\text{NH}_4\text{NO}_3$ . Compared with hydroponically grown plants, the secretion rate of xylem exudates was much lower in soil-grown plants, and secretion rates could not be precisely determined. However, in those cases when enough xylem sap could be collected over 1.5 h after decapitation of the shoot, the nitrate content of the xylem sap in the two mutants was found to be lower than that in the wild type (see Supplemental Figure 3 online). Thus, depending on the growth conditions, either the xylem sap nitrate concentration or the nitrate secretion rate into the xylem in the *nrt1.5* mutants was lower than that in the wild type.

The reduction in root-to-shoot translocation was specific to nitrate. As shown in Figure 5A, in the *nrt1.5-1* mutant, the shoot/

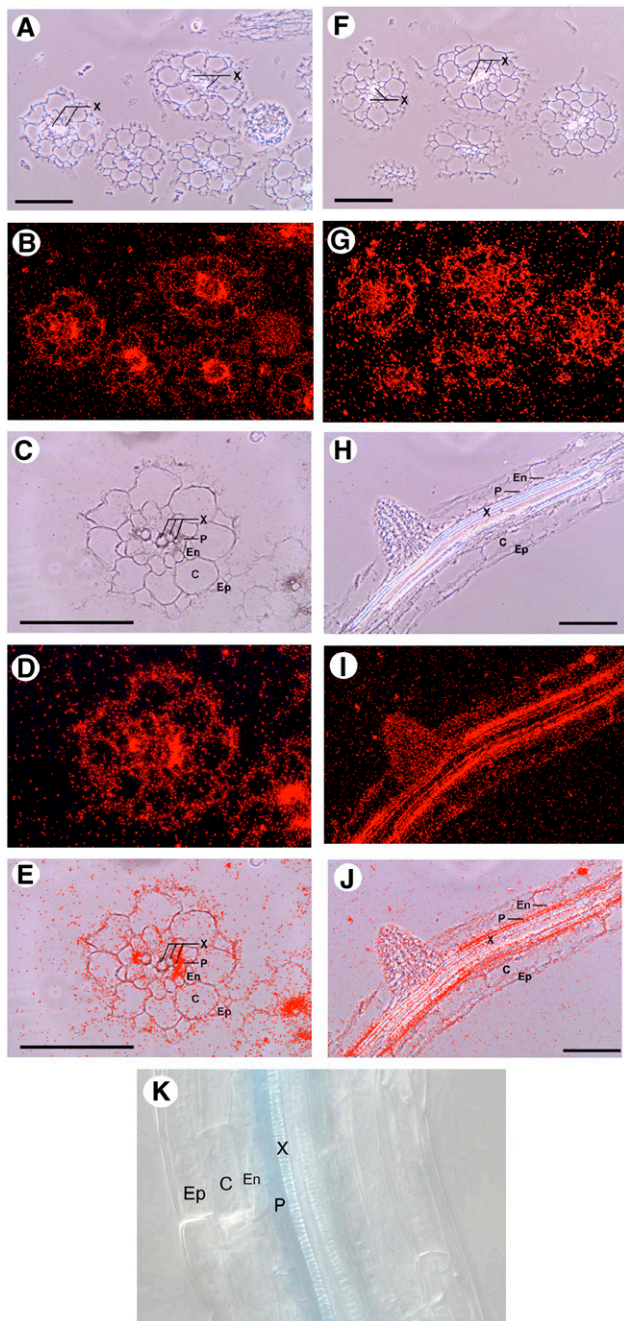


**Figure 6.** High Levels of *NRT1.5* Expression Are Seen in the Root Pericycle Cells Close to the Xylem.

(A) to (E) and (H) to (J) In situ hybridization of the antisense *NRT1.5* probe to a section of *Arabidopsis* root tissue.

(F) and (G) In situ hybridization of the sense *NRT1.5* probe to a section of *Arabidopsis* root tissue.

(A), (C), (F), and (H) Bright-field microscopy.

(B), (D), (G), and (I) Dark-field exposure using a colored filter causing the *NRT1.5* signal to appear as red.

(E) and (J) Merged bright-field exposure and dark-field exposure photographs.

(A) to (G) Cross sections of *Arabidopsis* root.

root  $^{35}\text{S}$  and  $^{33}\text{P}$  content ratio measured after 30 min exposure to 1 mM  $^{35}\text{SO}_4^{2-}$  (left panel) or 1 mM  $^{32}\text{PO}_4^{2-}$  (right panel) was similar to, or slightly higher than, that in the wild type. Together with the analysis of the antisense plants, the data for the T-DNA-tagged mutants demonstrate that *NRT1.5* plays an important role in root-to-shoot nitrate translocation.

To determine whether cation distribution was affected in the *nrt1.5* mutants, plants were grown in medium with either  $\text{NH}_4\text{NO}_3$  or  $(\text{NH}_4)_2$  succinate as the nitrogen source and then the shoot and root cation contents were analyzed by atomic absorption spectrophotometry. As shown in Figure 5B, when plants were grown in nitrate-containing medium, the amount of potassium transported to the shoot was reduced in the *nrt1.5-1* mutant, while the partition of calcium and magnesium was unchanged. However, when plants were grown in  $(\text{NH}_4)_2$  succinate medium, no difference was seen between the wild type and the *nrt1.5-1* mutant in the shoot/root partition of potassium, calcium, and magnesium (Figure 5B). Similar results for root-to-shoot potassium translocation were obtained for *nrt1.5-2* (see Supplemental Figure 4 online). These data show that the defect in the root-to-shoot translocation of potassium in *nrt1.5-1* and *nrt1.5-2* is nitrate specific.

Besides the defect in root-to-shoot nitrate translocation, the *nrt1.5* mutants also exhibited a morphological difference in root development. When the plants were grown in soil, no visible difference was observed between the wild type and mutants. However, when they were grown on plates, particularly with a high concentration of nitrate, the roots of the mutants were shorter than those of the wild type (see Supplemental Figure 5 online).

#### *NRT1.5* Is Expressed in Root Pericycle Cells Close to the Xylem

To investigate how *NRT1.5* is involved in root-to-shoot nitrate translocation, the spatial distribution of *NRT1.5* mRNA in root tissue was examined by in situ hybridization. As shown in Figures 6A to 6E, two clusters of silver grains (red in appearance due to a colored filter) were seen in cross sections of *Arabidopsis* root hybridized with the antisense probe. Since the row of xylem cells can be easily identified in bright-field microscopy, the clusters of silver grains were found at the periphery of the central vascular cylinder, especially in the area close to the protoxylem (Figures 6A and 6B). At higher magnification (Figures 6C to 6E), these clusters were found to be located between the endodermis and xylem, the region in which the pericycle cells are found (Figure 6E). No clusters were seen in cross sections hybridized with the sense probe (Figures 6F and 6G). In some longitudinal sections hybridized with the antisense probe, the high density of silver grains was seen as two continuous strips (Figures 6H to 6J). As shown in Figures 6I and 6J, one of the high-density strips was

(H) to (J) Longitudinal sections of *Arabidopsis* root.

(K) Histochemical localization of GUS activity in transgenic *Arabidopsis* plants expressing the GUS reporter gene under the control of the *NRT1.5* promoter region. Longitudinal view of the root. X, xylem; P, pericycle; En, endodermis; C, cortex; Ep, epidermis. Bars = 100  $\mu\text{m}$ .

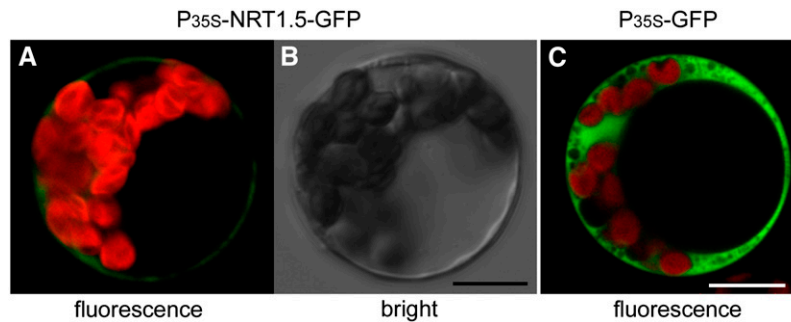


**Figure 7.** NRT1.5 is located in the Plasma Membrane.

(A) and (B) Representative microscopy images of an *Arabidopsis* protoplast expressing the NRT1.5-GFP fusion protein. (A) shows overlap of the GFP (green) and chlorophyll (red) fluorescence and (B) a bright-field image. GFP fluorescence was detected at the plasma membrane. (C) Protoplasts expressing GFP used as a control. Bars = 20  $\mu\text{m}$ .

disrupted by an emerging lateral root, and at this point, the xylem could be clearly visualized in the base of the lateral root, confirming that the site at which *NRT1.5* mRNA accumulated was external to the xylem. Since the lateral root is initiated from pericycle cells, disruption of the high-density strip by the lateral root supports the notion that *NRT1.5* is expressed in pericycle cells. These in situ hybridization analyses of cross sections and longitudinal sections of roots show that *NRT1.5* is expressed in the vascular system of the roots, especially in the pericycle cells close to the protoxylem.

In addition, localization of *NRT1.5* expression was analyzed in transgenic plants carrying the  $\beta$ -glucuronidase (*GUS*) gene under the control of the *NRT1.5* promoter (2.4 kb). Consistent with the in situ hybridization result, *GUS* activity was detected in the parenchyma cells (most likely the pericycle cells) close to the xylem vessels (Figure 6K). Consistent with our in situ localization and promoter-*GUS* assay results, transcriptome analysis of various root tissues by other authors (Birnbaum et al., 2003) also showed that *NRT1.5* is expressed predominantly in the pericycle.

### NRT1.5 Is Localized to the Plasma Membrane

To determine its subcellular location, *NRT1.5* was fused in frame with green fluorescent protein (GFP) and transiently expressed in *Arabidopsis* protoplasts under the control of the cauliflower mosaic virus 35S promoter. Analyses of *NRT1.5-GFP*-expressing *Arabidopsis* cells by confocal microscopy showed that the green fluorescence was confined to the plasma membrane (Figure 7A). Thus, NRT1.5 is a plasma membrane-localized nitrate transporter.

### NRT1.5 Can Transport Nitrate in Both Directions

The nitrate transporters of the NRT1 family from higher plants and the dipeptide transporters from bacteria, fungi, animals, and higher plants form a cotransporter family called NRT1(PTR) (for peptide transporter) (Paulsen and Skurray, 1994; Steiner et al., 1995; Tsay et al., 2007). In addition to nitrate and peptides, His uptake has been reported for two members of the NRT1/PTR

family, PHT1 from the rat and Bn NRT1.2 from *Brassica napus* (Yamashita et al., 1997; Zhou et al., 1998). NRT1.5 shares a higher degree of sequence identity with the *Arabidopsis* peptide transporters PTR2 (NTR1) and PTR1 (42 and 43%, respectively) (Rentsch et al., 1995; Song et al., 1996; Dietrich et al., 2004) than with the *Arabidopsis* nitrate transporters CHL1, NRT1.2, and NRT1.4 (36, 38, and 38%, respectively) (Tsay et al., 1993; Huang et al., 1999; Chiu et al., 2004). However, the function of the NRT1 (PTR) family cannot easily be inferred by sequence similarity (Lin et al., 2000).

To determine the function of NRT1.5, we performed electrophysiological analyses using the *Xenopus laevis* oocyte expression system. Two days after cRNA injection, oocytes were incubated at pH 7.4, voltage clamped at  $-60$  mV, and perfused with 10 mM substrate at the indicated pH. As shown in Figure 8A, a shift in pH from 7.4 to 5.5 in the absence of nitrate (control) elicited little current change in *NRT1.5*- or water-injected oocytes, whereas the inward current elicited by nitrate at pH 5.5 in *NRT1.5*-injected oocytes ( $37.6 \pm 15.3$  nA) was  $\sim 40$  times larger than that in water-injected controls ( $0.9 \pm 7.4$  nA). In contrast with the nitrate response, seven different dipeptides, as well as His, elicited little or no current change in At *NRT1.5*-injected oocytes at all membrane potentials tested from  $-160$  to 0 mV (Figures 8A and 8B). These data show that NRT1.5 is a nitrate transporter, as no transport activity was detected for His and the tested dipeptides.

As expected for a proton-coupled nitrate transporter with a proton/nitrate ratio larger than one, in the *NRT1.5*-injected oocytes, a net cation influx (i.e., an inward current or negative current) was elicited by the negatively charged nitrate, and the amplitude of the inward currents elicited by exposure to nitrate were pH dependent, being larger at pH 5.5 than at pH 7.4, while the currents elicited by nitrate at pH 7.4 were only  $\sim 30\%$  of those elicited at pH 5.5 (Figure 8B). The inward current elicited by external nitrate and the pH dependency of the elicited current suggest that NRT1.5 functions as a proton-coupled nitrate transporter, which mediates the influx of both nitrate and protons, with the proton/nitrate ratio being greater than one.

Our previous study showed that CHL1 (NRT1.1) is a dual-affinity nitrate transporter, as *CHL1*-injected oocytes exhibit

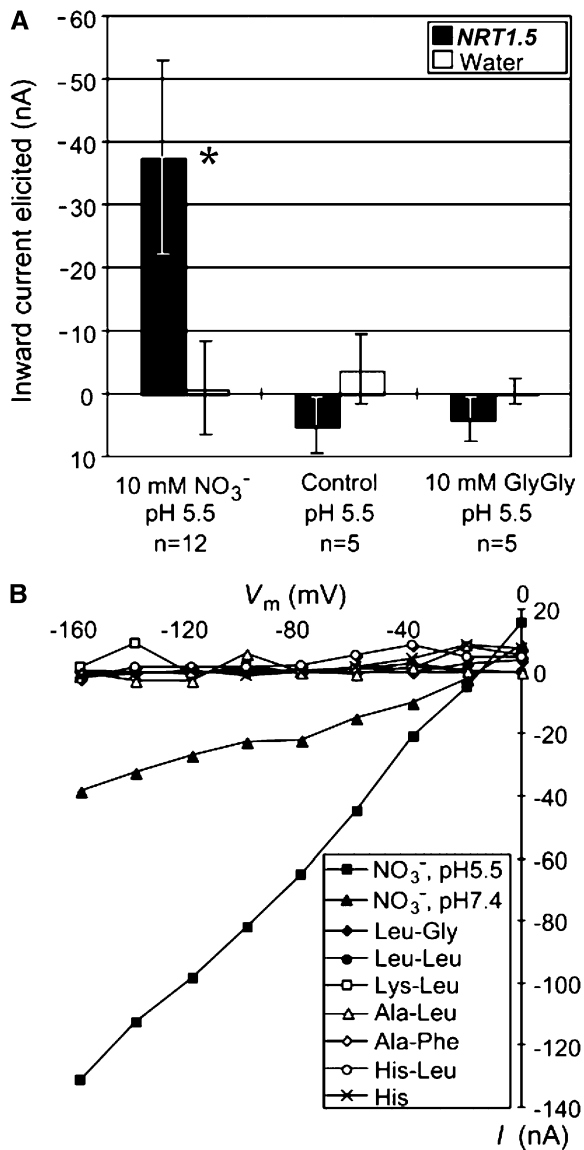


**Figure 8.** NRT1.5 Can Transport Nitrate but Not Dipeptides.

**(A)** Averages of the currents elicited by the indicated solutions in oocytes injected with *NRT1.5* cRNA or water. Oocytes were incubated at pH 7.4, voltage clamped at  $-60$  mV, and then perfused with control solution (no substrate) or with 10 mM substrate (nitrate or dipeptide GlyGly) at pH 5.5. n, number of oocytes tested from four different frogs; \*,  $P < 0.01$  compared with the water-injected control.

**(B)** Current-to-voltage relationship for NRT1.5. The  $I$ - $V$  curves were determined as described previously (Huang et al., 1999). The curves presented were recorded from a single *NRT1.5*-injected oocyte treated with 10 mM nitrate at pH 5.5 (closed squares), 10 mM nitrate at pH 7.4 (closed triangles), or Leu-Gly (closed diamonds), Leu-Leu (closed circles), Lys-Leu (open squares), Ala-Leu (open triangles), Ala-Phe (open diamonds), His-Leu (open circles), or His (indicated by an X) all at 10 mM and pH 5.5. Similar results were obtained in three other oocytes isolated from two different frogs.

uptake activity in both the low-affinity (10 mM) and high-affinity (250  $\mu$ M) concentration range (Liu et al., 1999; also shown in Figure 9). By contrast, low-affinity (Figure 9A), but not high-affinity (Figure 9B), nitrate uptake activity was observed in *NRT1.5*-injected oocytes. To determine the affinity of NRT1.5 for nitrate, *NRT1.5*-injected oocytes were exposed to different concentrations of nitrate at pH 5.5. As shown in Figure 9C, the amplitude of the inward current elicited at  $-60$  mV was concentration dependent. The  $K_m$  value, calculated for membrane potentials from  $-150$  to  $-30$  mV, was relatively constant at 5 to 6 mM (Figure 9D). This shows that, like NRT1.2 (Huang et al., 1999) and Os NRT1.1 (Lin et al., 2000), NRT1.5 is a low-affinity nitrate transporter but not a dual-affinity transporter, with a  $K_m$  of  $\sim 6$  mM.

To determine whether NRT1.5 could mediate nitrate efflux,  $^{15}\text{NO}_3^-$  was injected into *NRT1.5*- or water-injected oocytes. As shown in Figure 10, after 4.5 h incubation in nitrate-free ND96 buffer at pH 7.4, the amount of nitrate retained in water-injected oocytes was essentially unchanged, while in *NRT1.5*-injected oocytes, it was reduced to  $\sim 60\%$  of the original levels, indicating that NRT1.5 can facilitate nitrate efflux. A recent study showed that another of the 53 *Arabidopsis* *NRT1(PTR)* genes, *NAXT1* (At3g45650), can mediate nitrate efflux (Segonzac et al., 2007).

To determine how the efflux activity of NRT1.5 is regulated,  $^{15}\text{NO}_3^-$ -injected oocytes were incubated in solutions with different proton or nitrate concentrations. Efflux activity was observed when the oocytes were incubated at pH 7.4 but not at pH 5.5 (Figure 10), suggesting that the efflux is either regulated by the external pH or requires a proton gradient. Similarly, a high concentration of nitrate (100 mM) in the external solution inhibited the efflux activity (Figure 10). On the other hand, a potassium gradient was not sufficient to facilitate nitrate export, as when oocytes were exposed to a similar potassium gradient at pH 7.4 and 5.5, no efflux activity was observed at pH 5.5; therefore, NRT1.5 does not export nitrate by a potassium-coupled mechanism. The effect of the pH gradient on the export activity of NRT1.5 was further analyzed by incubating oocytes at various pH levels from 5.5 to 7.5. As shown in Supplemental Figure 6 online, the export activity of NRT1.5 increased with an increase in pH. Together, these results of the electrophysiological current measurement and  $^{15}\text{NO}_3^-$  efflux assay indicate that NRT1.5 can transport nitrate in both directions, probably via a proton-coupled mechanism.

## DISCUSSION

### NRT1.5 Is Important for the Efficient Long-Distance Transport of Nitrate

Nitrate content analysis of antisense plants and  $^{15}\text{N}$  partition analysis of two independent knockout mutants demonstrated that the *nrt1.5* mutants were defective in transporting nitrate from the root to shoot but showed essentially normal nitrate uptake. Consistent with the mutant phenotype, functional analysis in *Xenopus* oocytes showed that NRT1.5 is an electrogenic, pH-dependent, low-affinity nitrate transporter, while in situ RNA hybridization, promoter-GUS analysis, and subcellular localization

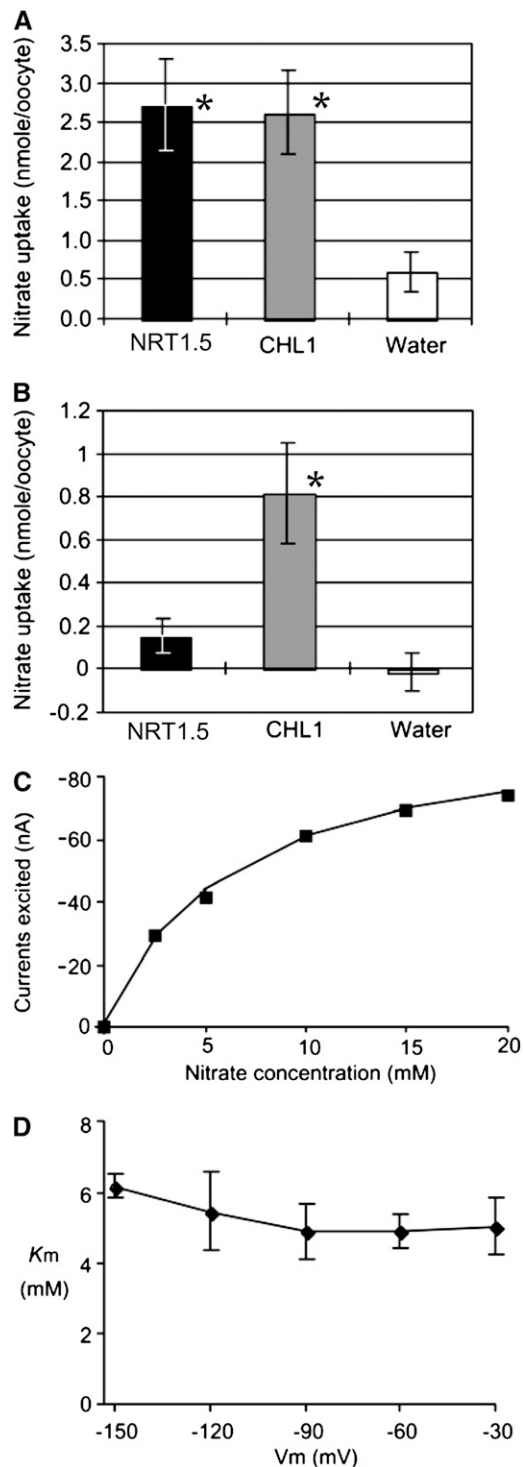


**Figure 9.** NRT1.5 Is a Low-Affinity Nitrate Transporter.

**(A)** Low-affinity nitrate uptake activity. Oocytes were incubated for 3 h with 10 mM nitrate, pH 5.5, and nitrate retained in the oocyte was measured by HPLC. \*,  $P < 0.01$  compared with the water-injected control.

**(B)** High-affinity nitrate uptake activity. Oocytes were incubated for 3 h with 250  $\mu$ M nitrate, pH 5.5, and then the amount of nitrate removed from the medium was determined by HPLC. Each data point represents the

studies showed that it is a plasma membrane protein expressed in the pericycle cells adjacent to the protoxylem. Together, these results show that NRT1.5 is involved in the xylem transport of nitrate.

The results of the oocyte  $^{15}\text{NO}_3^-$  efflux assay and the pH dependence of the efflux activity indicated that NRT1.5 can facilitate nitrate export, probably by a proton-coupled mechanism. Thus, our data indicate that NRT1.5 is responsible for exporting nitrate out of the pericycle cells into the xylem. Because of the negative membrane potential, nitrate is expected to be exported passively out of pericycle cells into the xylem. However, a role for NRT1.5 in xylem loading suggests an unexpected, but interesting, model in which proton-coupled nitrate export is involved in xylem loading. The involvement of a proton-coupled nitrate transporter in xylem loading implies that there is a regulatory link between root-to-shoot nitrate transport and xylem pH.

NRT1.5 is not the first proton-coupled transporter shown to be capable of bidirectional transport. Using the giant patch clamp techniques, Carpaneto et al. (2005) showed that the maize proton-coupled sucrose carrier SUT1 can transport sucrose into and out of the cell, depending on the direction of the sucrose and pH gradient and the membrane potential, suggesting that it is responsible for sucrose uptake into the phloem in mature leaves and for sucrose export from the phloem vessels in sink tissue. Thus, these studies on SUT1 and NRT1.5 indicate that proton-coupled transporters can function as export systems in higher plants.

#### The Pericycle Cells Close to the Protoxylem Play a Special Role in Controlling Xylem Loading

Similar to NRT1.5, several channels and transporters known to be involved in xylem loading or its regulation are expressed in pericycle cells close to the protoxylem. Examples are the outward potassium channel SKOR (Gaymard et al., 1998), the efflux-type boron transporter BOR1 (Takano et al., 2002), the tonoplast sulfate transporters SULTR4;1 and SULTR4;2 (Kataoka et al., 2004b), the plasma membrane sulfate transporters, SULTR2;1

average value from measurements on eight batches, each of five oocytes. Similar results were obtained with oocytes isolated from two other frogs. \*,  $P < 0.01$  compared with the water-injected control.

**(C)** Concentration dependence of nitrate-elicited currents in a single injected oocyte. The oocyte was voltage-clamped at  $-60$  mV, and the currents elicited by nitrate, pH 5.5, were plotted as a function of the external nitrate concentration. In this particular experiment, the  $K_m$ , calculated by fitting to the Michaelis-Menten equation using a nonlinear least-squares method in the Origin 5.0 program (Microcal Software), was  $6.1 \pm 0.5$  mM, and the average  $K_m$  calculated from three independent oocytes was  $5.6 \pm 0.4$  mM.

**(D)** Voltage dependence of the  $K_m$  for nitrate at pH 5.5. Oocytes were voltage-clamped at  $-60$  mV and subjected to voltage pulses between  $-30$  mV and  $-150$  mV for 300 ms with a  $-30$  mV increment. The  $K_m$  values were determined by fitting the current elicited at each voltage to the Michaelis-Menten equation. Shown here are the average values of the  $K_m$  calculated from three oocytes from different frogs.

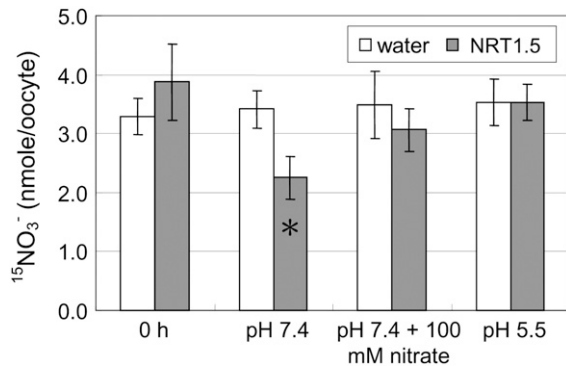


**Figure 10.** Oocyte Studies Show That NRT1.5 Can Export Nitrate.

$^{15}\text{NO}_3^-$  was injected into oocytes previously injected with NRT1.5 cRNA or water as a control, and the amount of  $^{15}\text{NO}_3^-$  in the oocytes determined immediately after injection (0 h) or after 4.5 h of incubation in nitrate-free ND96 buffer at pH 7.4 or 5.5 or in a buffer containing 100 mM  $\text{KNO}_3$  at pH 7.4. The data shown are the average and SD for the results from five oocytes from the same frog. Similar results were obtained using five other batches of oocytes from different frogs. \*,  $P < 0.01$  compared with the water-injected control and the 0 h control.

and SULTR3;5 (Kataoka et al., 2004a), PHO1 (Hamburger et al., 2002), and the citrate transporter FRD3 (Green and Rogers, 2004; Durrett et al., 2007). Uptake and xylem loading are two critical steps in regulating the amounts and types of ions available for shoot growth. However, compared with uptake, much less is known about ion xylem loading and regulation due to the difficulty in accessing nonepidermal cells for electrophysiological analysis. Now that these molecular markers important for xylem loading have been identified, GFP reporter lines can be generated and the protoplast of the pericycle cells close to the protoxylem isolated using a fluorescence-activated cell sorter (Birnbaum et al., 2005) and the xylem pole pericycle cells isolated can be used for patch clamping or expression analysis to provide insights into the molecular mechanism and the regulation of xylem loading.

### Multiple Xylem Loading Systems

Knockout of NRT1.5 expression did not completely eliminate root-to-shoot nitrate transport (Figure 4D; see Supplemental Figure 2 online), suggesting that, like nitrate uptake, nitrate xylem loading also involves multiple mechanisms and that NRT1.5 is responsible for one of these. Knockdown of NRT1.5 expression in the wild type had a profound effect on root-to-shoot nitrate transport (Figure 3C, anti-NRT1.5 #1 and #2), whereas knockdown of expression in the *chl1* (*nrt1.1*) deletion mutant had no effect (Figure 3C, anti-NRT1.5 #4 and #5). Since CHL1 (NRT1.1), which is involved in uptake, is expressed in the epidermis, cortex, and endodermis (Huang et al., 1996), while NRT1.5 is expressed in pericycle cells, it is unlikely that there is a direct interaction between NRT1.1 and NRT1.5, in contrast with the situation with SULTR2;1 and SULTR3;5, which probably form a heterodimer (Kataoka et al., 2004a). The different behaviors of NRT1.5 in the

wild type and *chl1* mutant might be due to differences in the tissue nitrate contents, since, as shown in Figure 3C, the tissue nitrate content of the *chl1* mutant was about one-third of that in the wild type. In other words, NRT1.5, with a  $K_m$  of  $\sim 6$  mM, could be responsible for the low-affinity xylem loading system, and, as with uptake, there might also be a higher affinity xylem loading system. In the *chl1* mutant, the tissue nitrate content is low, and, consequently, nitrate xylem loading is mainly mediated by the high-affinity system. This could explain the observation that knockdown of NRT1.5 expression in the *chl1* (*nrt1.1*) background did not result in decreased root-to-shoot nitrate transport (Figure 3C).

A similar concentration-dependent phenomenon has been reported in the *pho1* mutant (Poirier et al., 1991). When the phosphate concentration in the medium is  $< 200$   $\mu\text{M}$ , phosphate transfer to the shoots of the *pho1* mutant is reduced to 3 to 10% of the wild type level, while, in plants grown in medium containing 1 mM phosphate, it is higher (50% more) than in the wild type, suggesting that PHO1 is important for high-affinity phosphate xylem loading and that there is some compensatory effect between the high-affinity and low-affinity loading systems. With multiple xylem loading systems, plants have more flexibility to regulate the amounts of ions delivered to the shoots.

### Diurnal Regulation of NRT1.5 Expression

NRT1.5 transcript levels peaked at the night-to-day transition and fell to a minimum at the day-to-night transition (Figure 2C). This diurnal pattern suggests that the xylem loading rate of nitrate is high in the light period but low in the dark period. Indeed, several studies have shown that root-to-shoot nitrate translocation rates are high in the day and low in the night (Macduff and Bakken, 2003; Siebrecht et al., 2003). Thus, in addition to the high transpiration rate, the high xylem loading rate in the light period could lead to the pronounced diurnal variation in the nitrate translocation rate. In leaves, the activity of nitrate reductase, the first enzyme in nitrate assimilation, also shows a diurnal rhythm, rising to a maximum during the first half of the light period (Scheible et al., 1997; Lillo et al., 2001). This high nitrate translocation rate during the daytime ensures sufficient nitrate supply for the shoot. It is worth noting that the transcriptional levels of nitrate reductase and NRT1.5 show identical diurnal changes, being highest at the night-to-day transition and lowest at the day-to-night transition. It would be interesting to know whether the diurnal variation in nitrate reductase and NRT1.5 transcripts are coordinately regulated by the same signaling network.

### Interaction between Nitrate and Potassium at the Step of Xylem Transport

Interestingly, in the two *nrt1.5* mutants, root-to-shoot potassium transport was reduced and the reduction was nitrate dependent (Figure 5B; see Supplemental Figure 3 online). The results of the oocyte efflux assay suggested that nitrate export by NRT1.5 is mediated by a proton-coupled mechanism and not by a potassium-coupled mechanism (Figure 10). The root-to-shoot potassium transport defect in the *nrt1.5* mutants could therefore be caused by reduced nitrate transport, rather than by a direct

involvement of NRT1.5 in potassium xylem loading. In addition, *NRT1.5* mRNA levels were downregulated when potassium was limiting (Figure 2B), suggesting that root-to-shoot nitrate transport is controlled by potassium levels. Conversely, microarray analyses have shown that the expression of a potassium xylem loading gene, *SKOR*, is upregulated by nitrate (Wang et al., 2004). These data suggest the presence of a regulatory loop at the level of xylem transport that maintains the balance between nitrate and potassium.

## METHODS

### Cloning and Sequence Analysis of NRT1.5

*NRT1.5* (At1g32450) was identified by a homology search of the EST database for *Arabidopsis thaliana* using the *CHL1* (*NRT1.1*) amino acid sequence. Using the EST clone identified (clone ID 36F6T7) as a probe, a full-length clone (*pAtNRT1.5*) was isolated from an *Arabidopsis* cDNA library (Elledge et al., 1991) constructed in the  $\lambda$ YES vector. To isolate the genomic clone of *NRT1.5*, *Arabidopsis* genomic DNA was subjected to *Sau3A* partial digestion and then ligated into  $\lambda$ DASH II (Stratagene) and the genomic library screened using *NRT1.5* cDNA as a probe. Subsequently, a 5-kb *XhoI* fragment containing the whole coding region and the 1.2-kb 5' upstream region of *NRT1.5* was subcloned and sequenced. Sequence comparison of *NRT1.5* with other members of the NRT1 (PTR) family (Tsay et al., 2007) was performed using the Genetics Computer Group program (version 10.0) with a gap penalty of 8 and a gap length penalty of 2.

### RNA Gel Blot Analysis

For nitrate induction analysis, as described previously (Huang et al., 1999), plants were grown vertically under continuous illumination on agarose plates with 2.5 mM  $(\text{NH}_4)_2$  succinate at pH 6.5 for 9 d, shifted to fresh plates with 2.5 mM  $(\text{NH}_4)_2$  succinate at pH 6.0 for 24 h, and then transferred to plates with 5 mM  $\text{KNO}_3$  or 5 mM KCl for the indicated time. Total RNA was extracted by grinding frozen tissues with TRIzol reagent (Gibco BRL). Hybridization was performed in buffer containing 5 $\times$  SSC (1 $\times$  SSC is 150 mM sodium chloride and 15 mM sodium citrate, pH 7), 5 $\times$  Denhardt's solution (1 $\times$  Denhardt's solution is 0.02% Ficoll, 0.02% PVP, and 0.02% BSA), 0.5% SDS, and 25  $\mu\text{g}/\text{mL}$  of single-stranded DNA. The membrane was washed with 2 $\times$  SSC at room temperature for 20 min and then with 2 $\times$  SSC, 0.1% SDS for 30 min and 0.2 $\times$  SSC, 0.1% SDS for 30 min. The 1.7-kb 5' portion of *NRT1.5* was used to synthesize the DNA or RNA probe for RNA gel blot analysis. When the DNA probe was used, the hybridization and wash were performed at 65°C; when the RNA probe was used, both were performed at 75°C.

### Antisense Construct and Plant Transformation

The 1.6-kb 5' portion from the 5' untranslated region to the second *Bgl*II site of *NRT1.5* cDNA was inserted in the opposite orientation between the cauliflower mosaic virus 35S promoter and the nopaline synthase terminator of the binary vector pBI121 using *SacI* and *Bgl*III to generate the cDNA fragment and *SacI* and *Bam*HI to generate the vector fragment. The antisense construct produced, pAs-AtNRT1.5, was introduced into wild-type and *chl1-5* (*nrt1.1-5*) plants using *Agrobacterium tumefaciens* (strain C58)-mediated in-the-plant vacuum infiltration (Bechtold et al., 1993). Transformants were selected on Murashige and Skoog plates containing kanamycin (50 mg/L) and confirmed by genomic DNA gel blot analyses. The homozygous progenies of three independent transgenic plants on the wild-type background (#1, #2, and #3) and two on the *chl1-5*

background (#4 and #5) were used for nitrate uptake and nitrate content analyses. The number of inserts was one in AS#1, #2, and #4, three in #3, and two in #5.

### Isolation and Characterization of Two T-DNA-Tagged Mutants, *nrt1.5-1* and *nrt1.5-2*

The *nrt1.5-1* mutant was isolated from the ALPHA population (*Ws* ecotype) of T-DNA-tagged *Arabidopsis* plants generated by the Arabidopsis Knockout Facility at the University of Wisconsin (Krysan et al., 1999). The primers used for PCR screening were the T-DNA left border primer JL202 (5'-CATTTTATAATAACGCTGCGGACATCTAC-3') and the *NRT1.5* reverse primer (5'-GTTGTATAGTTTGTACCATTTTGCACAT-3'), which will amplify a 3.5-kb DNA fragment in the mutant. The second mutant, *nrt1.5-2* (SALK\_005099), was obtained from the European Arabidopsis Stock Center. Genomic PCR analysis and DNA gel blot analyses of genomic DNA digested with various restriction enzymes and probed with *NptII* (kanamycin resistance gene) showed that there was only a single copy of T-DNA inserted in the second intron of the *NRT1.5* gene. RT-PCR was performed as described previously (Chiu et al., 2004) using the forward primer (5'-AACGTCGACACGATGAAGAAGAAAGAA-3') and the reverse primer (5'-TTGGTCGACTTTAGAATCCTTCTCTCG-3').

### Nitrate Uptake Assay Using HPLC

The basal nutrient solution A without nitrogen consisted of 10 mM  $\text{K}_2\text{HPO}_4$ - $\text{KH}_2\text{PO}_4$ , 2 mM  $\text{MgSO}_4$ , 0.1 mM  $\text{FeSO}_4$ -EDTA, 1 mM  $\text{CaCl}_2$ , 50  $\mu\text{M}$   $\text{H}_3\text{BO}_3$ , 12  $\mu\text{M}$   $\text{MnSO}_4\cdot\text{H}_2\text{O}$ , 1  $\mu\text{M}$   $\text{ZnCl}_2$ , 1  $\mu\text{M}$   $\text{CuSO}_4\cdot 5\text{H}_2\text{O}$ , 0.2  $\mu\text{M}$   $\text{NaMoO}_4\cdot 2\text{H}_2\text{O}$ , 1 g/L of MES, 0.5% sucrose, 1 mg/L of thiamine, 100 mg/L of inositol, 0.5 mg/L of pyridoxine, and 0.5 mg/L of nicotinic acid.

For the uptake assay, seeds were surface-sterilized and sown in a 125-mL flask containing the nutrient solution A with 12.5 mM  $\text{NH}_4\text{NO}_3$  as nitrogen source at pH 5.5. The plants were grown under continuous illumination and rotated at 80 rpm at 25°C for 2 weeks. To measure uptake activity, the plants were washed three times with 10 mM  $\text{K}_2\text{HPO}_4$ - $\text{KH}_2\text{PO}_4$ , pH 5.5, and then shifted to 30 mL of nutrient solution A containing 8 mM  $\text{KNO}_3$ , pH 5.5. Nitrate uptake activity was measured by the amount of nitrate left in the solution at the indicated time determined using HPLC (Huang et al., 1999).

### Nitrate Content Analysis Using HPLC

For nitrate content analysis, surface-sterilized seeds were sown on nylon netting supported by a raft in a culture vessel (Magenta) as described previously (Touraine and Glass, 1997) and grown for 1 week in the nutrient solution A described above containing 12.5 mM  $\text{NH}_4\text{NO}_3$  and then shifted to fresh medium containing 12.5 mM  $(\text{NH}_4)_2$  succinate for 1 week. When plants are grown sterilely on lifted mesh with gentle shaking, the shoots are not exposed to the liquid medium, and ammonium will not be converted into nitrate by bacteria contamination. To determine nitrate partition between the shoots and roots, the plants were washed and shifted to fresh nutrient solution A containing 8 mM  $\text{KNO}_3$  for 16 h and then nitrate in the root and shoot was extracted in boiling water and determined as described previously (Chiu et al., 2004).

### Nitrate Uptake Assay Using $^{15}\text{NO}_3^-$

Plants were grown for 10 d on nylon netting supported by a raft as described above in the nutrient solution A containing 5 mM  $\text{NH}_4\text{NO}_3$  at pH 6, washed in 0.1 mM  $\text{CaSO}_4$  for 1 min, and transferred to fresh nutrient solution containing 4 mM  $\text{NH}_4^{15}\text{NO}_3$  with a 99% atom excess of  $^{15}\text{N}$  for 5, 30, or 180 min.  $^{15}\text{N}$  content was analyzed using a continuous-flow isotope ratio mass spectrometer coupled with a carbon nitrogen elemental analyzer (ANCA-GSL 20/20; PDZ Europa).

### Nitrate Content Analysis Using $^{15}\text{NO}_3^-$

Plants at the vegetative stage were grown hydroponically. The basal nutrient solution B without nitrogen consisted of 1 mM  $\text{KH}_2\text{PO}_4$ , 1 mM  $\text{MgSO}_4$ , 250  $\mu\text{M}$   $\text{CaCl}_2$ , 0.1 mM Na-Fe-EDTA, 50  $\mu\text{M}$  KCl, 50  $\mu\text{M}$   $\text{H}_3\text{BO}_3$ , 5  $\mu\text{M}$   $\text{MnSO}_4$ , 1  $\mu\text{M}$   $\text{ZnSO}_4$ , 1  $\mu\text{M}$   $\text{CuSO}_4$ , and 0.1  $\mu\text{M}$   $(\text{NH}_4)_6\text{Mo}_7\text{O}_{24}$ , pH adjusted to 6 with KOH. The plants were cultivated for 8 weeks in a 10-liter tank (Lejay et al., 1999) with the environmental parameters of light/dark cycle 8/16 h, light intensity 300  $\mu\text{mol}\cdot\text{s}^{-1}\cdot\text{m}^{-2}$  PAR, temperature 22°C/20°C, and 70% humidity. The nutrient solution was renewed twice a week for the first 7 weeks of culture and daily for the last week.

Root influx of  $\text{NO}_3^-$  was then assayed according to Delhon et al. (1995). The plants were transferred to 0.1 mM  $\text{CaSO}_4$  for 1 min, then to complete nutrient solution B containing  $^{15}\text{NO}_3^-$  with a 99% atom excess of  $^{15}\text{N}$  for short-term labeling (5 or 30 min) or a 20% atom excess of  $^{15}\text{N}$  for long-term labeling (180 min). At the end of labeling, the roots were washed for 1 min in 0.1 mM  $\text{CaSO}_4$  and separated from the shoots. The organs were dried at 70°C for 48 h, weighed, and analyzed for total  $^{15}\text{N}$  content using a continuous-flow isotope ratio mass spectrometer coupled with a carbon nitrogen elemental analyzer (ANCA-MS; PDZ Europa) as described by Clarkson et al. (1996).

### S and P Partition Analysis of Plants Labeled with $^{35}\text{SO}_4^{2-}$ or $^{33}\text{PO}_4^{3-}$

Measurement of the  $^{35}\text{S}$  and  $^{33}\text{P}$  distribution was performed using the same principle as the  $^{15}\text{N}$  uptake measurement. The roots were rinsed for 1 min in 0.1 mM  $\text{CaSO}_4$ , and then the plants were labeled for 30 min in nutrient solution B containing either  $^{33}\text{PO}_4^{3-}$  or  $^{35}\text{SO}_4^{2-}$ . The specific activities of the tracers were  $2.11\cdot 10^{11}$  dpm $\cdot\text{mol}^{-1}$  for  $^{33}\text{P}$  and  $7.24\cdot 10^{11}$  dpm $\cdot\text{mol}^{-1}$  for  $^{35}\text{S}$ . Roots and shoots are collected after  $2 \times 1$  min washes in 0.1 mM  $\text{CaSO}_4$ . Dry matter was weighed and ions extracted in 0.1 N HCl for 24 h at 4°C. Radioactivity was measured in scintillation liquid (Ultima Gold; Packard) using a scintillation counter (Tricarb 2100TR; Packard).

### Potassium, Calcium, and Magnesium Partition Analysis

Plants were grown on lifted nylon netting in nutrient solution A as described above, with either 12.5 mM  $\text{NH}_4\text{NO}_3$  or 12.5 mM  $(\text{NH}_4)_2$  succinate as the nitrogen source. The potassium, calcium, and magnesium contents of the roots and shoots were analyzed as described previously (Chiu et al., 2004).

### In Situ Hybridization

Plants were grown vertically for 2 weeks on agarose nutrient plates containing 12.5 mM  $(\text{NH}_4)_2$  succinate, pH 6.5 (Huang et al., 1999) and then were shifted to medium with 25 mM  $\text{KNO}_3$ , pH 5.5, for 16 h before harvesting the root tissues for fixation. Tissues were fixed and processed as described by Huang et al. (1999).  $^{35}\text{S}$ -labeled *NRT1.5* antisense (or sense) RNA was synthesized using T3 (or T7) RNA polymerase from *Spel* (or *KpnI*)-linearized pKS-AtNRT1.5 [pBluescript II KS+ (Stratagene) containing the 2.1-kb *EcoRI* fragment of *NRT1.5* cDNA, from which the poly (A) tail had been removed]. Root sections were hybridized with the hydrolyzed RNA probes and washed as described previously (Jackson, 1991; McKhann and Hirsch, 1993) and the slides coated with Kodak NTB-2 emulsion (International Biotechnologies) and exposed for 1 month at 4°C.

### Promoter-GUS Analysis

A 1.4-kb genomic fragment containing the promoter region and 30 bp of the coding region of *NRT1.5* was isolated by PCR and cloned in front of, and in frame with, the GUS gene in the binary vector pBI121. Plant transformation was performed as described above. Six-day-old seed-

lings grown on plates with 25 mM  $\text{KNO}_3$  (Huang et al., 1999) were harvested and vacuum-infiltrated in prefix solution (0.5% formaldehyde, 0.05% Triton X-100, and 50 mM sodium phosphate, pH 7) at room temperature for 1.5 h. After three washes in 50 mM sodium phosphate, pH 7, the seedlings were incubated in X-Gluc staining solution (50 mM sodium phosphate, pH 7, 0.05% Triton X-100, 1 mM potassium ferrocyanide, 1 mM potassium ferricyanide, and 1 mM 5-bromo-4-chloro-3-indoyl- $\beta$ -D-glucuronide) at 37°C in the dark for 3 h. After three washes in 50 mM sodium phosphate, pH 7, the seedlings were again fixed overnight in 2% formaldehyde, 0.5% glutaraldehyde, 100 mM sodium phosphate, pH 7, and GUS activity was analyzed visually using a Zeiss microscope.

### GFP Fusion and Subcellular Localization

To construct the cDNA encoding the translational fusion between *NRT1.5* and GFP, *NRT1.5* cDNA was amplified using the primers At NRT1.5 G5B (5'-CCCGGATCCAAATGCTTGCCTAGAGATT-3') and At NRT1.5 G3B (5'-GGGGATCCAGACTTTAGAAATCCTTCTCTC-3'), which removes the stop codon and introduces *Bam*HI restriction sites. The *NRT1.5* cDNA was then cloned into the *Bam*HI site of the plant transient expression vector 326-GFP (Lee et al., 2001) to generate a construct coding for a fusion protein with GFP in the C-terminal under the control of the cauliflower mosaic virus 35S promoter. The *NRT1.5*-GFP fusion construct or the vector 326GFP was transiently expressed in *Arabidopsis* protoplasts.

### *Arabidopsis* Protoplast Transformation

Plasmids were purified using Qiagen columns according to the manufacturer's protocol. *Arabidopsis* protoplasts were prepared from leaf tissues of 3- to 4-week-old plants grown on soil and the fusion constructs introduced by polyethylene glycol-mediated transformation as described previously (Sheen, 2001). *Arabidopsis* mesophyll protoplasts were resuspended in W5 medium (154 mM NaCl, 125 mM  $\text{CaCl}_2$ , 5 mM KCl, and 2 mM MES, pH 5.7) containing 5 mM glucose and 0.5 mM  $\text{KNO}_3$ . Fluorescent cells were imaged by confocal microscopy (Zeiss LSM510) with excitation at 488 nm. The fluorescence emission signals were detected using a band-pass filter of 505 to 530 nm for GFP and a long-pass filter of 650 nm for the far-red autofluorescence of chloroplasts.

### Functional Analysis of *NRT1.5* in *Xenopus laevis* Oocytes

The 2-kb *NRT1.5* cDNA was cloned into the oocyte expression vector *pGEMHE* (Liman et al., 1992). Capped mRNA was transcribed in vitro using mMMESSAGE mMACHINE kits (Ambion). Oocytes were isolated and injected with 50 ng of *NRT1.5* cRNA in 50 nL of water as described previously (Tsay et al., 1993), except that the Barth solution was replaced with ND96 solution (96 mM NaCl, 2 mM KCl, 1 mM  $\text{MgCl}_2$ , 1.8 mM  $\text{CaCl}_2$ , and 5 mM HEPES, pH 7.4). The oocytes were then incubated for 2 d in ND96 solution containing 10 mg/L of gentamicin before recording. Current measurements were recorded as described previously (Huang et al., 1999). High- and low-affinity nitrate uptake assays of injected oocytes using HPLC analysis were performed as described previously (Liu et al., 1999).

For nitrate efflux measurement, oocytes were microinjected with 50 nL of  $\text{K}^{15}\text{NO}_3$  (100 mM) with a 99% atom excess of  $^{15}\text{N}$  and then incubated for 4.5 h in ND96 buffer, pH 7.4 or 5.5, or in 100 mM  $\text{KNO}_3$ , 1 mM  $\text{MgCl}_2$ , 1.8 mM  $\text{CaCl}_2$ , and 5 mM HEPES, pH 7.4. At 0 h (immediately after  $\text{K}^{15}\text{NO}_3$  injection) or after 4.5 h of incubation, oocytes were washed three times with ND96 buffer and then dried at 70°C overnight before analysis for total  $^{15}\text{N}$  content using a continuous-flow isotope ratio mass spectrometer coupled with a carbon nitrogen elemental analyzer (ANCA-GSL MS; PDZ Europa).

### Accession Numbers

Sequence data from this article can be found in the Arabidopsis Genome Initiative or GenBank/EMBL databases under the following accession numbers: At1g32450 (NRT1.5), At1g12110 (CHL1, NRT1.1), At1g69850 (NRT1.2), At2g26690 (NRT1.4), At3g54140 (PTR1), At2g02040 (PTR2), At1g08090 (NRT2.1), At1g08100 (NRT2.2), At5g44340 (TUB4), At4g05320 (UBQ10), Os03g13274 (Os NRT1.1), U17987 (Bn NRT1.2), and AB000280 (rat PHT1).

### Supplemental Data

The following materials are available in the online version of this article.

**Supplemental Figure 1.** At *NRT1.5* Expression Is Downregulated by Potassium Limitation.

**Supplemental Figure 2.** Root-to-Shoot <sup>15</sup>N Translocation Defect of the T-DNA-Inserted *nrt1.5-2* Mutant.

**Supplemental Figure 3.** Nitrate Concentration of Xylem Sap of Plants Grown in Soil Is Reduced in *nrt1.5* Mutants.

**Supplemental Figure 4.** Potassium Translocation Is Reduced in *nrt1.5-2*.

**Supplemental Figure 5.** Growth Phenotype of *nrt1.5* Mutants.

**Supplemental Figure 6.** Export Activity of At NRT1.5 Is pH Dependent.

**Supplemental Data Set 1.** Text File Corresponding to Figure 1.

### ACKNOWLEDGMENTS

This work was supported by grants from the Institute of Molecular Biology, Academia Sinica, Taiwan, and the National Science Council (NSC 97-2311-B-001-009) to Y.-F.T. We thank the English editor Thomas Barkas for comments and suggestions.

Received April 23, 2008; revised August 28, 2008; accepted September 2, 2008; published September 9, 2008.

### REFERENCES

- Bechtold, N., Ellis, J., and Pelletier, G.C.R. (1993). In planta Agrobacterium mediated gene transfer by infiltration of adult Arabidopsis thaliana plants. *C. R. Acad. Sci. Paris* **316**: 1194–1199.
- Birnbaum, K., Shasha, D.E., Wang, J.Y., Jung, J.W., Lambert, G.M., Galbraith, D.W., and Benfey, P.N. (2003). A gene expression map of the Arabidopsis root. *Science* **302**: 1956–1960.
- Birnbaum, K., Jung, J.W., Wang, J.Y., Lambert, G.M., Hirst, J.A., Galbraith, D.W., and Benfey, P.N. (2005). Cell type-specific expression profiling in plants via cell sorting of protoplasts from fluorescent reporter lines. *Nat. Methods* **2**: 615–619.
- Canvin, D.T., and Atkins, C.A. (1974). Nitrate, nitrite and ammonia assimilation by leaves: Effect of light, carbon dioxide and oxygen. *Planta* **116**: 207–224.
- Carpaneto, A., Geiger, D., Bamberg, E., Sauer, N., Fromm, J., and Hedrich, R. (2005). Phloem-localized, proton-coupled sucrose carrier ZmSUT1 mediates sucrose efflux under the control of the sucrose gradient and the proton motive force. *J. Biol. Chem.* **280**: 21437–21443.
- Chiu, C.-C., Lin, C.-S., Hsia, A.-P., Su, R.-C., Lin, H.-L., and Tsay, Y.-F. (2004). Mutation of a nitrate transporter, AtNRT1:4, results in a reduced petiole nitrate content and altered leaf development. *Plant Cell Physiol.* **45**: 1139–1148.
- Clarkson, D.T., Gojon, A., Saker, L.R., Wiersema, P.K., Purves, J.V., Tillard, P., Arnold, G.M., Paams, A.J.M., Waalburg, W., and Stulen, I. (1996). Nitrate and ammonium influxes in soybean (*Glycine max*) roots: Direct comparison of <sup>13</sup>N and <sup>15</sup>N tracing. *Plant Cell Environ.* **19**: 859–868.
- Delhon, P., Gojon, A., Tillard, P., and Passama, L. (1995). Diurnal regulation of NO<sub>3</sub><sup>-</sup> uptake in soybean plants. I. Changes in NO<sub>3</sub><sup>-</sup> influx, efflux, and N utilization in the plant during the day/night cycle. *J. Exp. Bot.* **46**: 1585–1594.
- Dietrich, D., Hammes, U., Thor, K., Suter-Grotemeyer, M., Fluckiger, R., Slusarenko, A.J., Ward, J.M., and Rentsch, D. (2004). AtPTR1, a plasma membrane peptide transporter expressed during seed germination and in vascular tissue of Arabidopsis. *Plant J.* **40**: 488–499.
- Durrett, T.P., Gassmann, W., and Rogers, E.E. (2007). The FRD3-mediated efflux of citrate into the root vasculature is necessary for efficient iron translocation. *Plant Physiol.* **144**: 197–205.
- Elledge, S.J., Mulligan, J.T., Ramer, S.W., Spottswood, M., and Davis, R.W. (1991). Lambda YES: A multifunctional cDNA expression vector for the isolation of genes by complementation of yeast and *Escherichia coli* mutations. *Proc. Natl. Acad. Sci. USA* **88**: 1731–1735.
- Filleur, S., Dorbe, M.F., Cerezo, M., Orsel, M., Granier, F., Gojon, A., and Daniel-Vedele, F. (2001). An Arabidopsis T-DNA mutant affected in *NRT2* genes is impaired in nitrate uptake. *FEBS Lett.* **489**: 220–224.
- Gaymard, F., Pilot, G., Lacombe, B., Bouchez, D., Bruneau, D., Boucherez, J., Michaux-Ferriere, N., Thibaud, J.-B., and Sentenac, H. (1998). Identification and disruption of a plant shaker-like outward channel involved in K<sup>+</sup> release into the xylem sap. *Cell* **94**: 647–655.
- Gilliham, M., and Tester, M. (2005). The regulation of anion loading to the maize root xylem. *Plant Physiol.* **137**: 819–828.
- Glass, A.D.M., Shaff, J.E., and Kochian, L.V. (1992). Studies of the uptake of nitrate in barley. *Plant Physiol.* **99**: 456–463.
- Glass, A.D.M., and Siddiqi, M.Y. (1995). Nitrogen absorption by plant roots. In *Nitrogen Nutrition in Higher Plants*, H.S. Srivastava and R.P. Singh, eds (New Delhi, India: Associated Publishing Co.), pp. 21–56.
- Green, L.S., and Rogers, E.E. (2004). FRD3 controls iron localization in Arabidopsis. *Plant Physiol.* **136**: 2523–2531.
- Guo, F.Q., Wang, R., Chen, M., and Crawford, N.M. (2001). The Arabidopsis dual-affinity nitrate transporter gene *AtNRT1.1* (*CHL1*) is activated and functions in nascent organ development during vegetative and reproductive growth. *Plant Cell* **13**: 1761–1777.
- Hamburger, D., Rezzonico, E., MacDonald-Comber Petetot, J., Somerville, C., and Poirier, Y. (2002). Identification and characterization of the Arabidopsis *PHO1* gene involved in phosphate loading to the xylem. *Plant Cell* **14**: 889–902.
- Huang, N.-C., Chiang, C.-S., Crawford, N.M., and Tsay, Y.-F. (1996). *CHL1* encodes a component of the low-affinity nitrate uptake system in Arabidopsis and shows cell type-specific expression in roots. *Plant Cell* **8**: 2183–2191.
- Huang, N.-C., Liu, K.-H., Lo, H.-J., and Tsay, Y.-F. (1999). Cloning and functional characterization of an Arabidopsis nitrate transporter gene that encodes a constitutive component of low-affinity uptake. *Plant Cell* **11**: 1381–1392.
- Jackson, D. (1991). In situ hybridization in plants. In *Molecular Plant Pathology*, D.J. Bowles, S.J. Gurr, and M. McPherson, eds (New York: Oxford University Press), pp. 163–174.
- Kataoka, T., Hayashi, N., Yamaya, T., and Takahashi, H. (2004a). Root-to-shoot transport of sulfate in Arabidopsis. Evidence for the role of SULTR3;5 as a component of low-affinity sulfate transport system in the root vasculature. *Plant Physiol.* **136**: 4198–4204.
- Kataoka, T., Watanabe-Takahashi, A., Hayashi, N., Ohnishi, M., Mimura, T., Buchner, P., Hawkesford, M.J., Yamaya, T., and Takahashi, H. (2004b). Vacuolar sulfate transporters are essential

- determinants controlling internal distribution of sulfate in Arabidopsis. *Plant Cell* **16**: 2693–2704.
- Köhler, B., and Raschke, K.** (2000). The delivery of salts to the xylem. Three types of anion conductance in the plasmalemma of the xylem parenchyma of roots of barley. *Plant Physiol.* **122**: 243–254.
- Köhler, B., Wegner, L.H., Osipov, V., and Raschke, K.** (2002). Loading of nitrate into the xylem: apoplastic nitrate controls the voltage dependence of X-QUAC, the main anion conductance in xylem-parenchyma cells of barley roots. *Plant J.* **30**: 133–142.
- Krysan, P.J., Young, J.C., and Sussman, M.R.** (1999). T-DNA as an insertional mutagen in Arabidopsis. *Plant Cell* **11**: 2283–2290.
- Lee, Y.-J., Kim, D.H., Kim, Y.-W., and Hwang, I.** (2001). Identification of a signal that distinguishes between the chloroplast outer envelope membrane and the endomembrane system in vivo. *Plant Cell* **13**: 2175–2190.
- Lejay, L., Tillard, P., Lepetit, M., Olive, F., Filleur, S., Daniel-Vedele, F., and Gojon, A.** (1999). Molecular and functional regulation of two NO<sub>3</sub><sup>-</sup> uptake systems by N- and C-status of Arabidopsis plants. *Plant J.* **18**: 509–519.
- Li, W., Wang, Y., Okamoto, M., Crawford, N.M., Siddiqi, M.Y., and Glass, A.D.** (2007). Dissection of the AtNRT2.1:AtNRT2.2 inducible high-affinity nitrate transporter gene cluster. *Plant Physiol.* **143**: 425–433.
- Lillo, C., Meyer, C., and Ruoff, P.** (2001). The nitrate reductase circadian system. The central clock dogma contra multiple oscillatory feedback loops. *Plant Physiol.* **125**: 1554–1557.
- Liman, E.R., Tytgat, J., and Hess, P.** (1992). Subunit stoichiometry of a mammalian K<sup>+</sup> channel determined by construction of multimeric cDNAs. *Neuron* **9**: 861–871.
- Lin, C.-M., Koh, S., Stacey, G., Yu, S.-M., Lin, T.-Y., and Tsay, Y.-F.** (2000). Cloning and functional characterization of a constitutively expressed nitrate transporter gene *OsNRT1* from rice. *Plant Physiol.* **122**: 379–388.
- Little, D.Y., Rao, H., Oliva, S., Daniel-Vedele, F., Krapp, A., and Malamy, J.E.** (2005). The putative high-affinity nitrate transporter NRT2.1 represses lateral root initiation in response to nutritional cues. *Proc. Natl. Acad. Sci. USA* **102**: 13693–13698.
- Liu, K.-H., Huang, C.-Y., and Tsay, Y.-F.** (1999). CHL1 is a dual-affinity nitrate transporter of Arabidopsis involved in multiple phases of nitrate uptake. *Plant Cell* **11**: 865–874.
- Liu, K.-H., and Tsay, Y.-F.** (2003). Switching between the two action modes of the dual-affinity nitrate transporter CHL1 by phosphorylation. *EMBO J.* **22**: 1005–1013.
- Loque, D., Tillard, P., Gojon, A., and Lepetit, M.** (2003). Gene expression of the NO<sub>3</sub><sup>-</sup> transporter NRT1.1 and the nitrate reductase NIA1 is repressed in Arabidopsis roots by NO<sub>2</sub><sup>-</sup>, the product of NO<sub>3</sub><sup>-</sup> reduction. *Plant Physiol.* **132**: 958–967.
- Macduff, J.H., and Bakken, A.K.** (2003). Diurnal variation in uptake and xylem contents of inorganic and assimilated N under continuous and interrupted N supply to *Phleum pratense* and *Festuca pratensis*. *J. Exp. Bot.* **54**: 431–444.
- McKhann, H.I., and Hirsch, A.M.** (1993). In situ localization of specific mRNAs in plant tissues. In *Methods in Plant Molecular Biology and Biotechnology*, B.R. Glick and J.E. Thompson, eds (Ann Arbor, MI: CRC Press), pp. 179–205.
- Munos, S., Cazettes, C., Fizames, C., Gaymard, F., Tillard, P., Lepetit, M., Lejay, L., and Gojon, A.** (2004). Transcript profiling in the chl1-5 mutant of Arabidopsis reveals a role of the nitrate transporter NRT1.1 in the regulation of another nitrate transporter, NRT2.1. *Plant Cell* **16**: 2433–2447.
- Paulsen, I.T., and Skurray, R.A.** (1994). The POT family of transport proteins. *Trends Biochem. Sci.* **19**: 404.
- Poirier, Y., Thoma, S., Somerville, C., and Schiefelbein, J.** (1991). Mutant of Arabidopsis deficient in xylem loading of phosphate. *Plant Physiol.* **97**: 1087–1093.
- Rentsch, D., Laloi, M., Rouhara, I., Schmelzer, E., Delrot, S., and Frommer, W.B.** (1995). NTR1 encodes a high affinity oligopeptide transporter in Arabidopsis. *FEBS Lett.* **370**: 264–268.
- Remans, T., Nacry, P., Pervent, M., Filleur, S., Diatloff, E., Mounier, E., Tillard, P., Forde, B.G., and Gojon, A.** (2006). The Arabidopsis NRT1.1 transporter participates in the signaling pathway triggering root colonization of nitrate-rich patches. *Proc. Natl. Acad. Sci. USA* **103**: 19206–19211.
- Scheible, W.R., Gonzalez-Fontes, A., Morcuende, R., Lauerer, M., Geiger, M., Glaab, J., Gojon, A., Schulze, E.D., and Stitt, M.** (1997). Tobacco mutants with a decreased number of functional nia genes compensate by modifying the diurnal regulation of transcription, post-translational modification and turnover of nitrate reductase. *Planta* **203**: 304–319.
- Segonzac, C., Boyer, J.C., Ipotesi, E., Szponarski, W., Tillard, P., Touraine, B., Sommerer, N., Rossignol, M., and Gibrat, R.** (2007). Nitrate efflux at the root plasma membrane: identification of an Arabidopsis excretion transporter. *Plant Cell* **19**: 3760–3777.
- Sheen, J.** (2001). Signal transduction in maize and Arabidopsis mesophyll protoplasts. *Plant Physiol.* **127**: 1466–1475.
- Siebrecht, S., Herdel, K., Schurr, U., and Tischner, R.** (2003). Nutrient translocation in the xylem of poplar-diurnal variations and spatial distribution along the shoot axis. *Planta* **217**: 783–793.
- Smirnov, N., and Stewart, G.R.** (1985). Nitrate assimilation and translocation by higher plants: Comparative physiology and ecological consequences. *Physiol. Plant.* **64**: 133–140.
- Song, W., Steiner, H.-Y., Zhang, L., Naider, F., Stacey, G., and Becker, J.M.** (1996). Cloning of a second Arabidopsis peptide transporter gene. *Plant Physiol.* **110**: 171–178.
- Steiner, H.-Y., Naider, F., and Becker, J.M.** (1995). The PTR family: A new group of peptide transporters. *Mol. Microbiol.* **16**: 825–834.
- Takano, J., Noguchi, K., Yasumori, M., Kobayashi, M., Gajdos, Z., Miwa, K., Hayashi, H., Yoneyama, T., and Fujiwara, T.** (2002). Arabidopsis boron transporter for xylem loading. *Nature* **420**: 337–340.
- Touraine, B., and Glass, A.D.M.** (1997). NO<sub>3</sub><sup>-</sup> and ClO<sub>3</sub><sup>-</sup> fluxes in the *chl1-5* mutant of *Arabidopsis thaliana*. *Plant Physiol.* **114**: 137–144.
- Tsay, Y.F., Chiu, C.C., Tsai, C.B., Ho, C.H., and Hsu, P.K.** (2007). Nitrate transporters and peptide transporters. *FEBS Lett.* **581**: 2290–2300.
- Tsay, Y.-F., Schroeder, J.I., Feldmann, K.A., and Crawford, N.M.** (1993). The herbicide sensitivity gene CHL1 of Arabidopsis encodes a nitrate-inducible nitrate transporter. *Cell* **72**: 705–713.
- Wang, R., Liu, D., and Crawford, N.M.** (1998). The Arabidopsis CHL1 protein plays a major role in high-affinity nitrate uptake. *Proc. Natl. Acad. Sci. USA* **95**: 15134–15139.
- Wang, R., Tischner, R., Gutierrez, R.A., Hoffman, M., Xing, X., Chen, M., Coruzzi, G., and Crawford, N.M.** (2004). Genomic analysis of the nitrate response using a nitrate reductase-null mutant of Arabidopsis. *Plant Physiol.* **136**: 2512–2522.
- Yamashita, T., Shimada, S., Guo, W., Sato, K., Kohmura, E., Hayakawa, T., Takagi, T., and Tohyama, M.** (1997). Cloning and functional expression of a brain peptide/histidine transporter. *J. Biol. Chem.* **272**: 10205–10211.
- Zhou, J.J., Fernandez, E., Galvan, A., and Miller, A.J.** (2000). A high affinity nitrate transport system from *Chlamydomonas* requires two gene products. *FEBS Lett.* **466**: 225–227.
- Zhou, J.-J., Theodoulou, F.L., Muldin, I., Ingemarsson, B., and Miller, A.J.** (1998). Cloning and functional characterization of a Brassica napus transporter that is able to transport nitrate and histidine. *J. Biol. Chem.* **273**: 12017–12023.

# Mutation of the Arabidopsis NRT1.5 Nitrate Transporter Causes Defective Root-to-Shoot Nitrate Transport

Shan-Hua Lin, Hui-Fen Kuo, Geneviève Canivenc, Choun-Sea Lin, Marc Lepetit, Po-Kai Hsu, Pascal Tillard, Huey-Ling Lin, Ya-Yun Wang, Chyn-Bey Tsai, Alain Gojon and Yi-Fang Tsay  
*PLANT CELL* 2008;20;2514-2528; originally published online Sep 9, 2008;  
DOI: 10.1105/tpc.108.060244

This information is current as of November 3, 2008

<b>Supplemental Data</b>	<a href="http://www.plantcell.org/cgi/content/full/tpc.108.060244/DC1">http://www.plantcell.org/cgi/content/full/tpc.108.060244/DC1</a>
<b>References</b>	This article cites 57 articles, 36 of which you can access for free at: <a href="http://www.plantcell.org/cgi/content/full/20/9/2514#BIBL">http://www.plantcell.org/cgi/content/full/20/9/2514#BIBL</a>
<b>Permissions</b>	<a href="https://www.copyright.com/ccc/openurl.do?sid=pd_hw1532298X&amp;issn=1532298X&amp;WT.mc_id=pd_hw1532298X">https://www.copyright.com/ccc/openurl.do?sid=pd_hw1532298X&amp;issn=1532298X&amp;WT.mc_id=pd_hw1532298X</a>
<b>eTOCs</b>	Sign up for eTOCs for <i>THE PLANT CELL</i> at: <a href="http://www.plantcell.org/subscriptions/etoc.shtml">http://www.plantcell.org/subscriptions/etoc.shtml</a>
<b>CiteTrack Alerts</b>	Sign up for CiteTrack Alerts for <i>Plant Cell</i> at: <a href="http://www.plantcell.org/cgi/alerts/ctmain">http://www.plantcell.org/cgi/alerts/ctmain</a>
<b>Subscription Information</b>	Subscription information for <i>The Plant Cell</i> and <i>Plant Physiology</i> is available at: <a href="http://www.aspb.org/publications/subscriptions.cfm">http://www.aspb.org/publications/subscriptions.cfm</a>